CHEMISTRY
A European Journal

Supporting Information

Synthesis and Isolation of the Titanium–Scandium Endohedral Fullerenes—$Sc_2TiC@I_h-C_{80}$, $Sc_2TiC@D_{5h}-C_{80}$ and $Sc_2TiC_2@I_h-C_{80}$: Metal Size Tuning of the Ti^{IV}/Ti^{III} Redox Potentials

Katrin Junghans,[a] Kamran B. Ghiassi,[b] Nataliya A. Samoylova,[a] Qingming Deng,[a] Marco Rosenkranz,[a] Marilyn M. Olmstead,*[b] Alan L. Balch,*[b] and Alexey A. Popov*[a]

chem_201601655_sm_miscellaneous_information.pdf

Supporting Information

Synthesis of fullerenes with CH_4, Ti, and Ti/CH_4

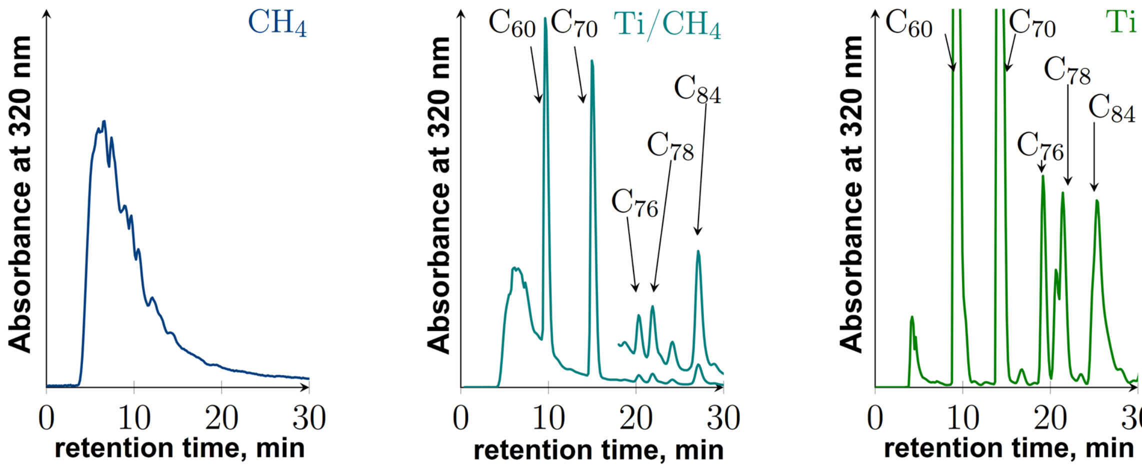

Figure S1a. HPLC chromatograms of raw fullerene mixtures synthesized in different conditions (Buckyprep column, toluene as eluent), from left to right: graphite/CH_4 (note the absence of well-defined peaks due to C_{60} and C_{70}), Ti-graphite/CH_4, and Ti-graphite without methane. In the Ti/CH_4 system, the yields of C_{60} and C_{70} are almost equal, whereas the distribution of higher fullerenes (retention times 20-30 min) is very different from that in Ti-graphite system or in standard empty fullerene synthesis (the latter two are very similar).

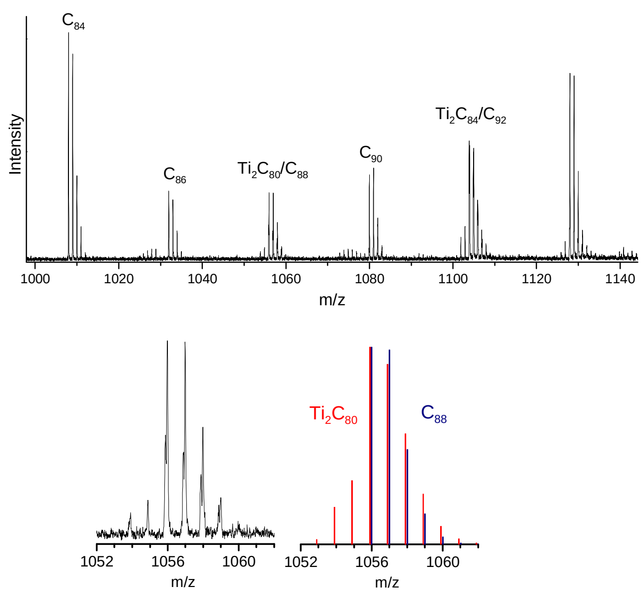

Figure S1b. Left: Mass-spectrum of the raw fullerene mixture from Ti synthesis. The spectra are dominated by empty fullerenes, but Ti_2C_{2n} structures can be also detected due to characteristic isotopic pattern of Ti. Right: experimental isotopic distribution for Ti_2C_{80}/C_{88} peaks compared to theoretical for Ti_2C_{80} (red) and C_{88} (dark blue).

Separation of $Sc_2TiC@C_{78}$

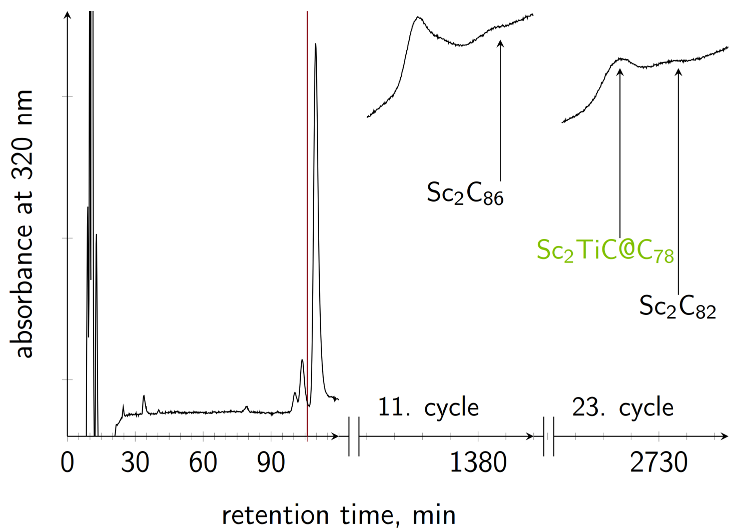

Figure S2. Fraction A (see Fig.1 in the manuscript) was subjected to recycling HPLC with Buckyprep column and toluene as eluent. Pure $Sc_2TiC@C_{78}$ was obtained after 23 cycles after removal of Sc_2C_{86} and Sc_2C_{82}.

Separation of $Sc_2TiC@I_h$-C_{80}

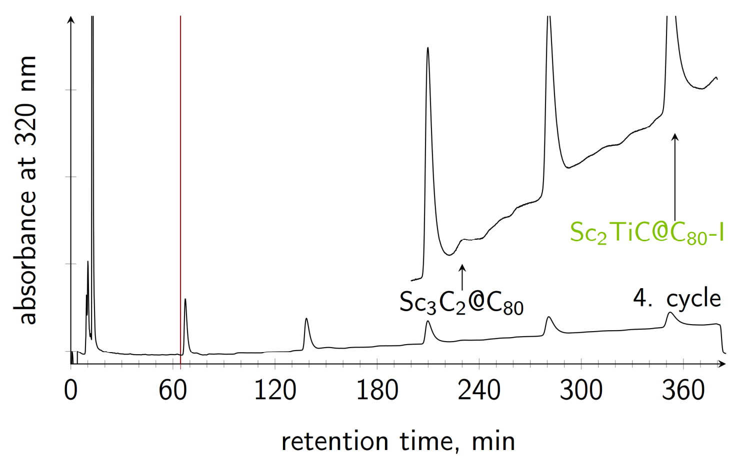

Figure S3. Fraction B was subjected to recycling HPLC with Buckyprep-M column and toluene as eluent. $Sc_3C_2@C_{80}$ (ca 15 % of the fraction) was removed after 4 cycles leaving pure $Sc_2TiC@I_h$-C_{80}.

$Sc_2TiC@C_{68}$

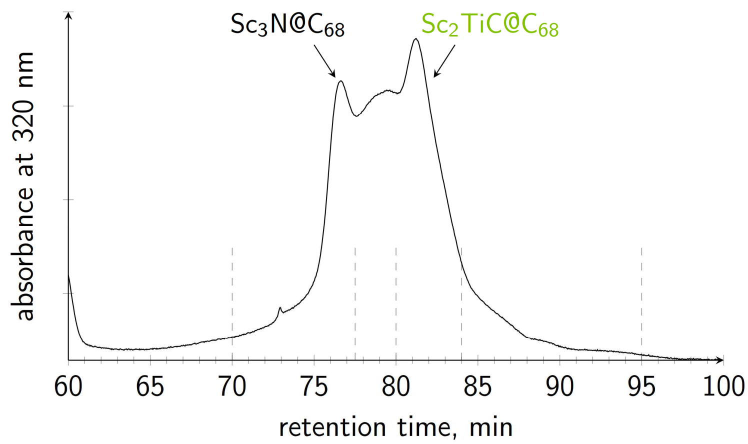

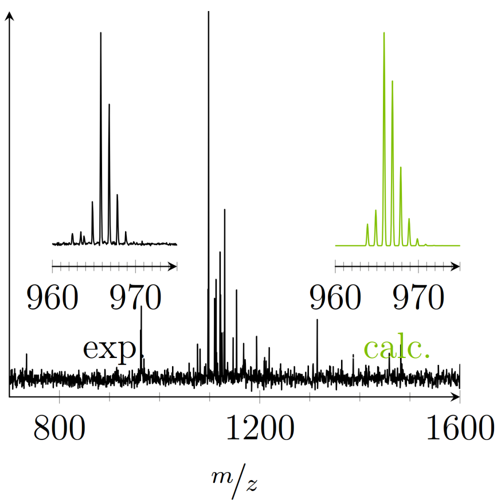

Figure S4. HPLC of the fraction containing $Sc_2TiC@C_{68}$ and $Sc_3N@C_{68}$ (4 Buckyperp columns, toluene as an eluent) and mass-spectrum of the fraction proving the presence of $Sc_2TiC@C_{68}$ (inset, peak maximum at 966). Low yield of the compound prevents its further separation.

$Sc_2TiC_2@C_{80}$-II

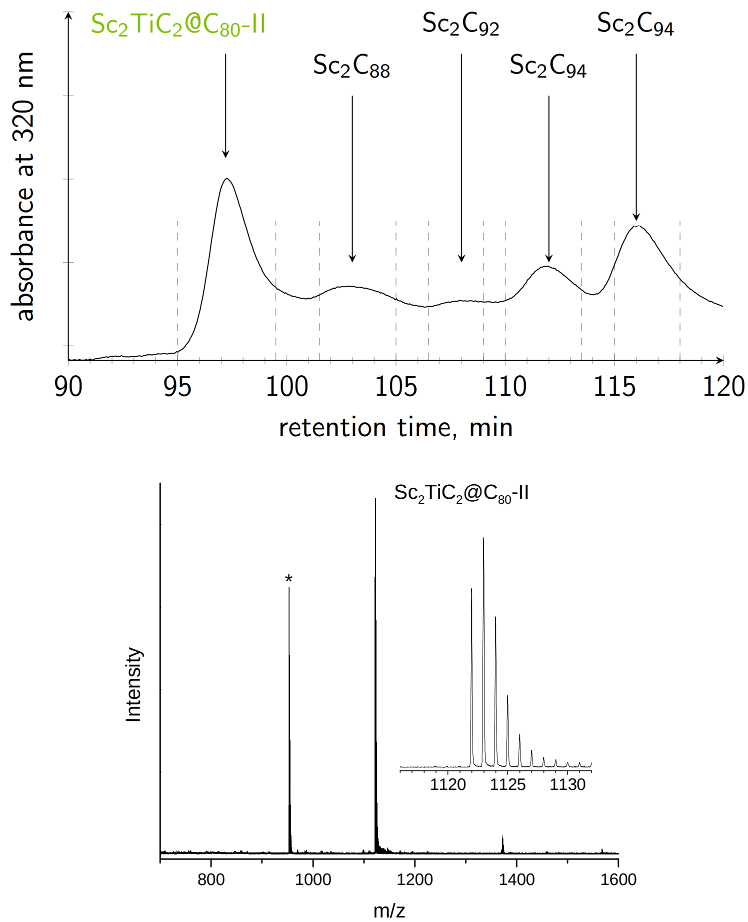

Figure S5. Top: HPLC curve of the fraction containing $Sc_2TiC_2@C_{80}$-II (4 Buckyperp columns, toluene as an eluent). Bottom: positive-ion MALDI mass-spectrum of the $Sc_2TiC_2@C_{80}$-II fraction (sulfur is used as a matrix, the feature marked with asterisk is due to the presence of matrix; note that the measurement were performed with ca 5% ^{13}C-enriched sample, hence isotopic distribution is differet from that shown in Fig. S6)

Mass-spectra of purified Sc-Ti carbide clusterfullerenes

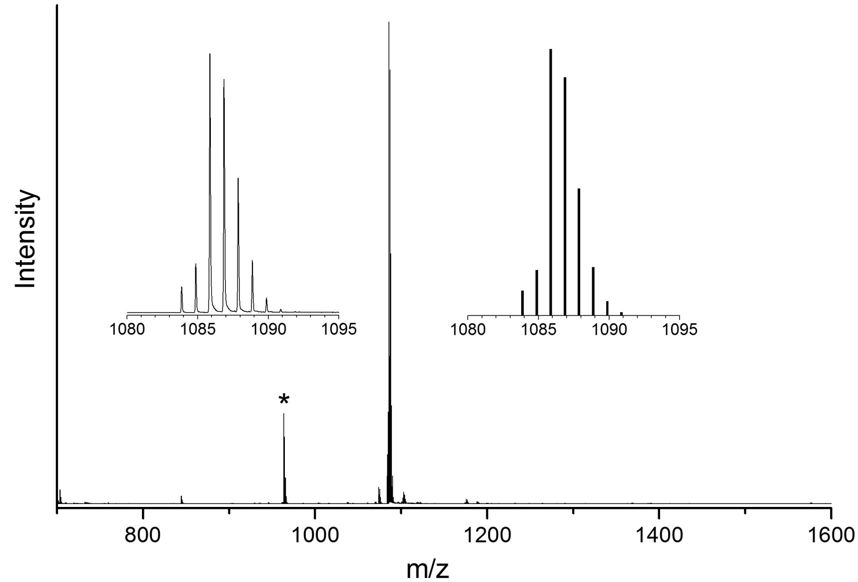

Figure S6a. Positive-ion MALDI Mass-spectrum of $Sc_2TiC@C_{78}$ (sulfur is used as a matrix, the feature marked with asterisk is due to the presence of matrix). Insets show experimental (left) and theoretical (right) isotopic distribution for $Sc_2TiC@C_{78}$.

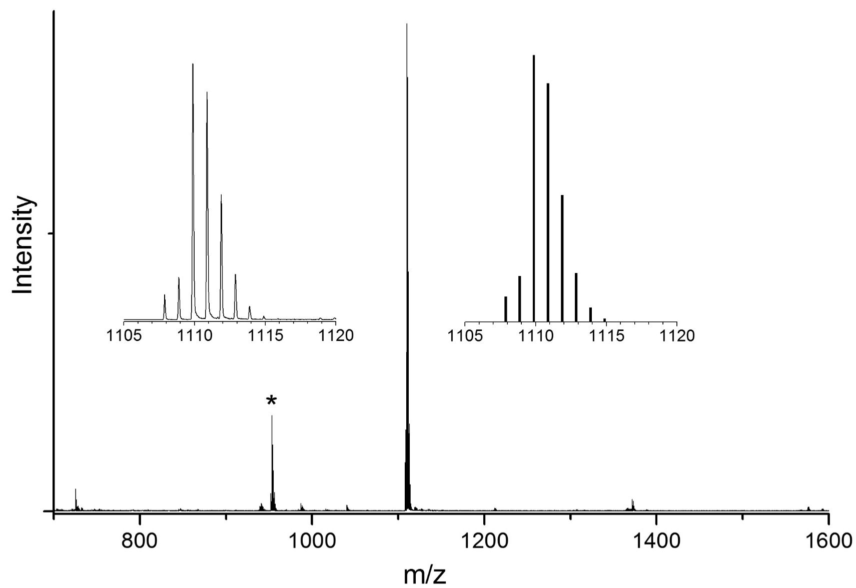

Figure S6b. Positive-ion MALDI Mass-spectrum of $Sc_2TiC@I_h\text{-}C_{80}$ (sulfur is used as a matrix, the feature marked with asterisk is due to the presence of matrix). Insets show experimental (left) and theoretical (right) isotopic distribution for $Sc_2TiC@C_{80}$.

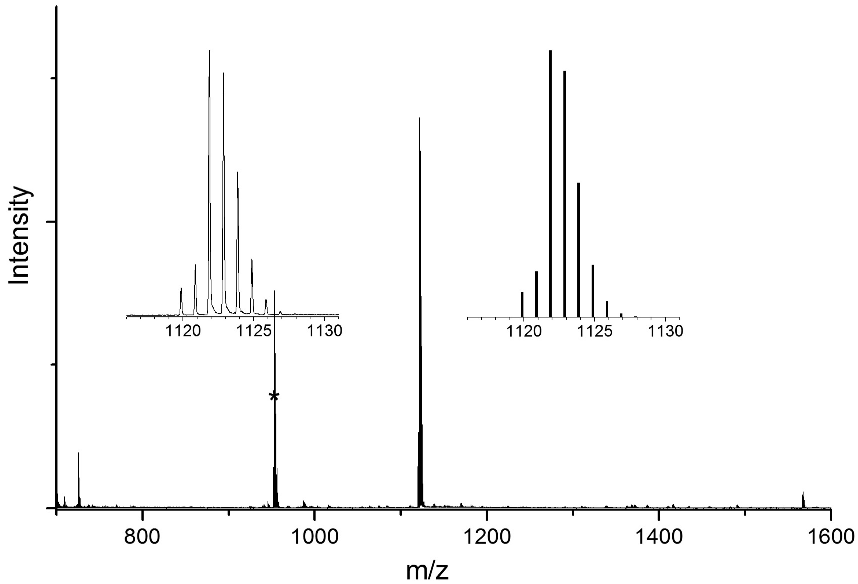

Figure S6c. Positive-ion MALDI Mass-spectrum of $Sc_2TiC_2@I_h$-C_{80} (sulfur is used as a matrix, the feature marked with asterisk is due to the presence of matrix). Insets show experimental (left) and theoretical (right) isotopic distribution for $Sc_2TiC_2@C_{80}$.

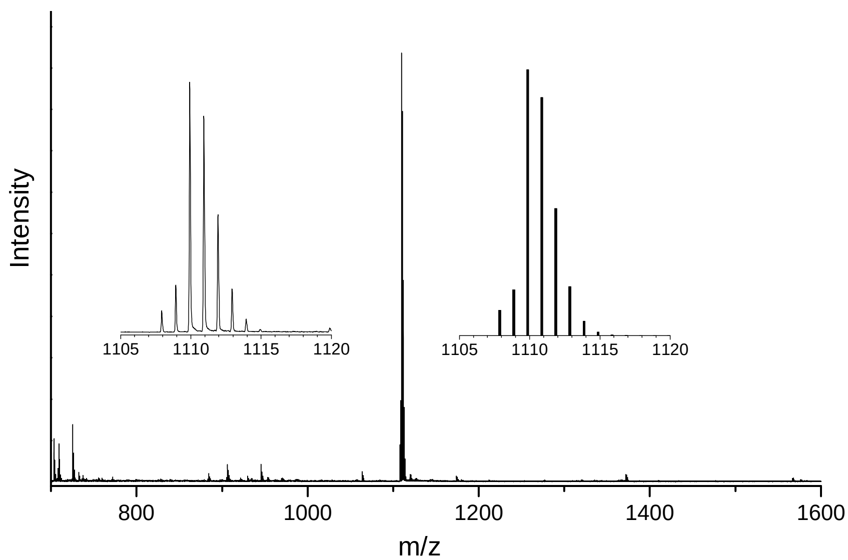

Figure S6d. Positive-ion MALDI Mass-spectrum of $Sc_2TiC@D_{5h}$-C_{80} (sulfur is used as a matrix). Insets show experimental (left) and theoretical (right) isotopic distribution for $Sc_2TiC@C_{80}$.

UV-Vis-NIR absorption spectra

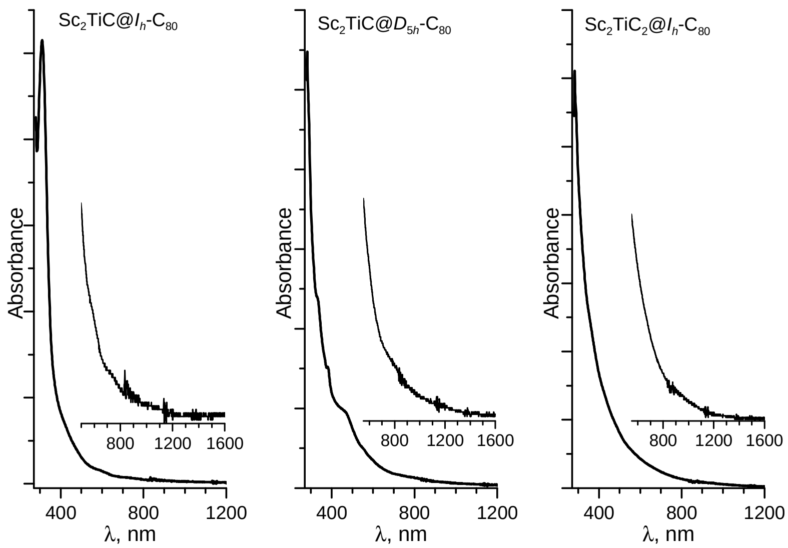

Figure 7a. UV-vis-NIR absorption spectra of $Sc_2TiC@I_h$-C_{80}, $Sc_2TiC@D_{5h}$-C_{80}, and $Sc_2TiC_2@I_h$-C_{80} in toluene solution. Insets show enhanced NIR region.

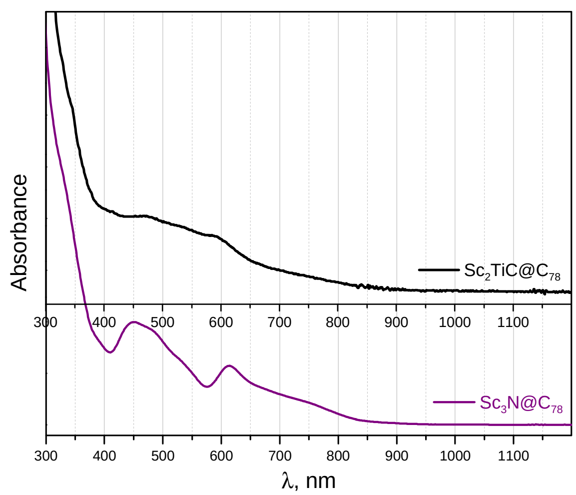

Figure 7b. UV-vis-NIR absorption spectrum of $Sc_2TiC@C_{78}$ in toluene compared to that of $Sc_3N@C_{78}$. Similarity of the spectra indicates that both EMFs may have the same carbon cage, $D_{3h}(5)$-C_{78}.

DFT-optimizes conformers of Sc_2TiC_2@I_h-C_{80}

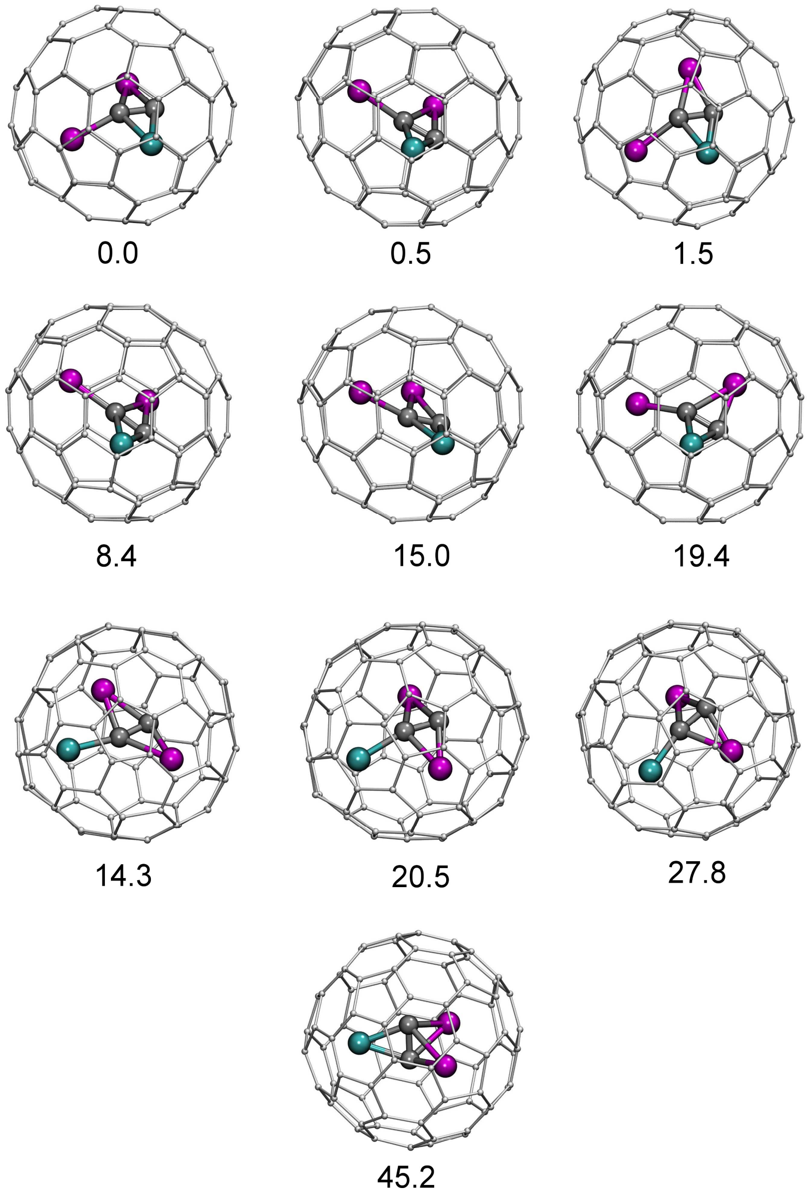

Figure 8. Selected DFT-optimized conformers of Sc_2TiC_2@I_h-C_{80}. Sc is magenta, Ti is cyan, endohedral carbons are dark grey. The value below each structure is its relative energy (in kJ/mol).

C_2 rearrangement in $Sc_2TiC_2@I_h$-C_{80}

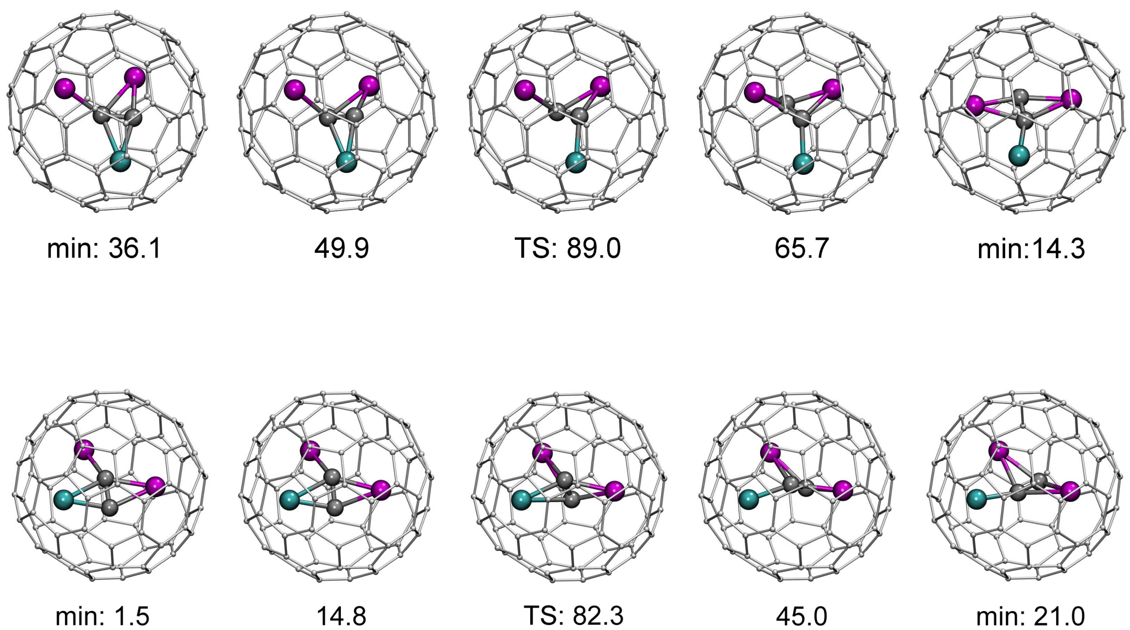

Figure 9. Selected structures on two intrinsic reaction coordinate (IRC) paths between two minima with different Ti-C_2 coordination (denoted as "min") via transition state (denoted "TS"); relative energies are in kJ/mol